METALURGI
Majalah Ilmu dan Teknologi
p-ISSN 0126-3188 | e-ISSN 2443-3926
ejurnalmaterialmetalurgi.lipi.go.id

EFFECT OF COOLING-MEDIUM INDUCED INITIAL STRUCTURE BEFORE INTERCRITICAL ANNEALING ON THE MICROSTRUCTURE AND MECHANICAL PROPERTIES OF LOW ALLOY DUAL-PHASE STEEL

Toni Bambang Romijarso[a,b*], Miftakhur Rohmah[a], Myrna Ariati[b], Efendi Mabruri[a], and Eddy Sumarno Siradj[b]

[a] Research Center for Metallurgy, National Research and Innovation Agency
Management Building 720, B.J. Habibie Sains and Technology Area, Banten, Indonesia 15314
[b]Department of Metallurgy and Materials Engineering, Universitas Indonesia
UI Campus, Kukusan, Depok, Jawa Barat, Indonesia 16425
*E-mail: toni001@brin.go.id

Received: 13-07-2023, Revised: 31-08-2023, Accepted: 11-09-2023

Abstract

The present research focused on determining the effect of cooling-medium-induced initial structure before the intercritical annealing induced dual-phase structure in the low alloy steel. Low carbon steel, which consists of containing 0.09 wt.% C was heated at 920 °C for 30 minutes to austenitization and then cooled in various media to provide the different initial structures before the IA (intercritical annealing) process. After austenization, the cooling process in the furnace and open-air provided a ferrite-pearlite phase, while the cooling process in water generated full martensite as the initial structure. Afterwards, the sample was intercritical-annealed at 750 °C (temperature between Ac1 and Ac3 lines or intercritical zone) for 10 minutes and then quenched in water. The water quenching after the austenitizing process improved the mechanical strength of steel (919 MPa), compared to the as-received state (519 MPa) due to martensite formation. As the cooling rate increased after the austenitizing process, the tensile strength increased and the elongation decreased. The different structures before intercritical annealing affected the martensite volume fraction and further correlated with improving mechanical properties. The ferrite and pearlite, as the initial structure before the IA process, provide a smaller fraction of martensite (18.36 vol.% for furnace cooling and 27.85 vol.% for open-air cooling). In contrast, the full martensite as the initial structure before IA generates a higher fraction of martensite (39.25 vol.%). The tensile strengths obtained were 512, 516, and 541 MPa with elongations of 29.8%, 30.1% and 32.6% for cooling furnace, open air and water, respectively. The strain-hardening behavior during the intercritical annealing is not affected by the initial process of the structure.

Keywords: *Dual-phase steel, intercritical anealing, low-alloy carbon steel, fraction of martensite*

1. INTRODUCTION

Dual-phase steel provides a superior mix of strength and ductility, more excellent weldability, an outstanding balance of strength and formability, and relatively easy processing methods due to its microstructure consisting of a matrix of ferrite and martensite/bainite phases. It has been widely utilized in the automobile industry, mainly passenger cars, since its development in 1970 [1]-[3]. When applied to vehicles, dual-phase steel was believed to reduce vehicles' weight and reduce exhaust emissions [4].

There are three primary methods for manufacturing DP (dual phase) steel: (1) direct intercritical heat treatment followed by water quenching (intercritical heat treatment-IHT), (2) austenitization and cooling into an intercritical

DOI : 10.55981/metalurgi.2023.727

Metalurgi is Sinta 2 Journal (https://sinta.kemdikbud.go.id/journals/profile/3708) accredited by Ministry of Education, Culture, Research, and Technology, Republic Indonesia

temperature zone followed by water quenching (continuous IHT), and (3) intercritical annealed of the quenched martensitic structure followed by water quench (IQ route) [4]. However, because of the varied initial microstructure formation, the morphological characteristics (including martensitic distribution, volume fraction, and grain size) of DP steel might be highly diverse.

Several previous researchers have studied the effect of initial microstructure on the mechanical properties of DP steel. The martensite and ferrite morphology can respond to the work hardening capacity, which improves mechanical properties [1]. Kalhor et al., [5] confirmed that the different initial microstructures significantly affect lath martensite distribution, mechanical properties (resulting in ~800 MPa), and fracture features of the 0.18C-0.14Si-1.29Mn steel. Jamei et al., [6] concluded that the rapid cooling before intercritical annealing on the 0.035C-0.268Mn-0.035Si steel provided a lower ratio between ultimate tensile strength and yield strength (UTS/YS) than the slow cooling.

Adamczyk's research (0.09C- 1.50Mn-0.014P-0.009S) found that the initial structure affects the martensite morphology in the dual-phase structure obtained [7]. But, the refined martensite island ~4.5 µm, which resulted from water quenched IHT process, enhanced the tensile strength and work hardening capacity. Contrarily, the refining grain with globular morphology was observed to improve the tensile strength without sacrificing ductility [1]. Besides that, the austenite distribution has significantly affected the morphology of the recrystallized ferrite grain and martensite evolution [8]. However, limited literature is reported to investigate the correlation of structure morphology on DP steel's mechanical and strain-hardening behavior. Besides controlling the heat treatment process, the carbon level on the austenitic phase also affected the martensite transformation behavior due to the changes in martensite start (Ms)temperature [9].

However, the intercritical annealing process of low-alloy steels has not been thoroughly studied. Adjusting the temperature and cooling rate after austenitization can control the initial structure's characteristics before intercritical annealling. Based on the previous research, the different cooling rate was provided by variations in cooling media. So, the focused present study evaluates the effect of the cooling-medium-induced initial structure after the austenitization on the microstructure transformation and its correlation with mechanical properties of low alloy steel when subjected to intercritical annealing.

2. MATERIALS AND METHODS

A low-alloy carbon steel sheet as-received with dimensions of 220 x 20 x 3 mm (length x width x thickness) was used in this study, which has the chemical composition presented in Table 1.

Table 1. Chemical composition of as-received low-alloy carbon steel (wt.%)

C	Si	Cr	Mn	Ni
0.0948	0.3651	0.5548	0.5839	0.0744
P	**S**	**Cu**	**Mo**	**V**
0.0064	0.0033	0.2445	0.0009	0.0004

The schematic of the dual-phase heat treatment process in the present study is displayed in Figure 1. Six samples were austenitized at 920 °C for 30 minutes to provide a full austenite structure. To generate a different initial microstructure before intercritical annealing, each sample was cooled at a different cooling rate using furnace cooling (annealed state), open-air cooling (normalizing), and water quenching. Afterward, the sample was re-heated to an intercritical annealing temperature (~750 °C) for 10 minutes to transform the dual-phase structure. This temperature was estimated in two zone (α+γ phase) by calculating the A_{c1} and A_{c3}, according to Haugardi Equation [9]-[10]:

$$A_{C1}(°C)=739-22C-7Mn+2Si+14Cr+13Mo-13Ni \quad (1)$$

$$A_{C3}(°C)=902-225C-11Mn-19Si-5Cr+13Mo-20Ni+55V \quad (2)$$

Based on Eq. 1-2 and chemical composition, the estimated A_{c1} and A_{c3} were 740 °C and 863 °C, respectively. Besides that, this steel's Ms (martensite start) can be calculated using the KE Thelning Equation, following Eq. 3 [10]. The result of the calculation of Ms is 486 °C.

$$Ms(°C) = 561-474C-33Mn-17Ni-17Cr-21Mo \quad (3)$$

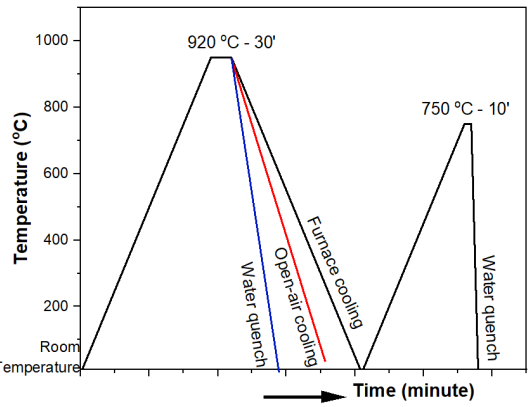

Figure 1. Schematic diagram of heat treatment process performed in this work

The metallographic observation was conducted to analyze the microstructure evolution during intercritical annealing. All samples were wet-ground by SiC paper with a roughness of 80 to 2000 grit. Then, sample was polished using a slurry of alumina powder (5, 3, 1, and 0.5 μm) to obtain the mirror-like surface. After that, the sample was etched into a 2% nitric acid solution (2% Nital). The metallographic test used an optical microscope (Olympus BX53M) and scanning electron microscope (JEOL JSM 639OA) for higher magnification. The grain size was calculated by Intercept method, according to ASTM E-112 [11]. GSN was grain size number and N_L was number of grain intercept.

$$GSN = 6.6439\, log_{10} N_L - 3.2877 \qquad (4)$$

Tensile and micro-vickers hardness test were used to confirm the effect of intercritical annealing on the mechanical properties. A tensile test was conducted at room temperature using the Tinnius Olsen 30 SL/Super L60 machine with a 25 mm/min cross-head speed. The specimens were prepared using wire cutting to obtain the dimension of sample sizes as shown in Fig. 2, according to ASTM E8/E8M-13a. While, the hardness test was carried out using the Mitutoyo HM 200 test equipment with a load of 1N and a loading time of 12 seconds. The hardness value was averaged from six position result.

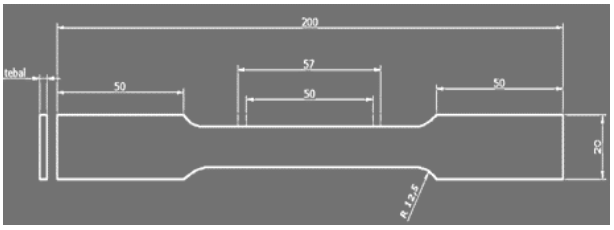

Figure 2. Dimension of tensile test carbon steel specimen

In the tensile test, the relationship between stress and strain is formulated as:

$$E = \sigma/\varepsilon \qquad (5)$$

Where E is the modulus of elasticity, σ is stress (MPa), and ε is strain (%). The strain hardening coefficient exponent (*n*) is a quantity that indicates the magnitude of the increase in strength and hardness due to plastic deformation.

The value of n flat metal specimens such as sheets or strips can be calculated from the force and extension data from the tensile test results of ASTM E8 / E8M -13a, using the general equation of flow stress σ with strain rate sensitivity (ASTM E 646), followed as Eq. 6.

$$\sigma = K.\varepsilon^{n} \qquad (6)$$

K is a material constant or strength coefficient [12]-[14]. Equation 5 has been corrected through a semi-logarithmic relationship [12]-[15].

3. Result and Discussion

3.1 Heat Treatment

Before experimenting, the TTT (time-temperature-transformation) and CCT (continuous cooling transformation) diagrams were simulated using JmatPro software to predict the microstructure evolution of the austenite phase after the austenitization process at 920 °C, depicted in Figure 3.

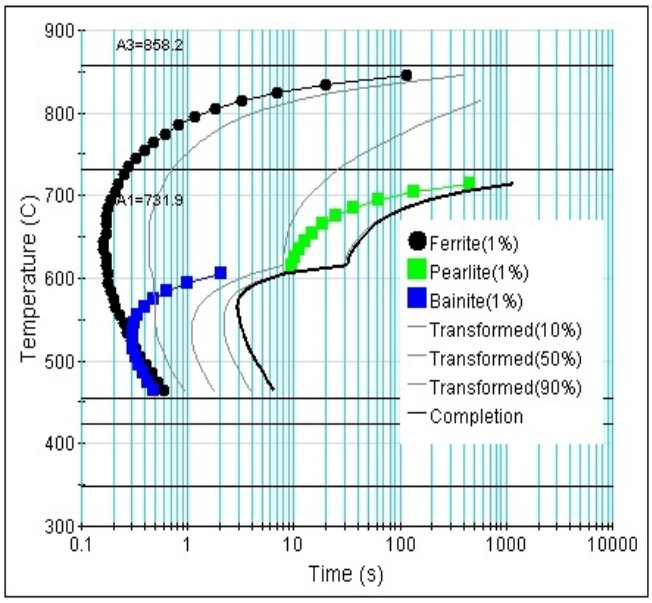

Figure 3. TTT diagram of tested steel

The intercritical zone was estimated at 731.9-858.2 °C, and the martensite was initially formed at 455 °C. Based on Figure 3, the time required for martensite formation is less than 1 minute, suggesting the cooling rate is very fast. Unfortunately, the ferrite also formed when the cooling time reached up to 0.2 s and was completed at 10-1000 s, concluding that slow cooling was required. In comparison, the pearlite transformation (green line) starts forming slower (10-1000s). According to the theory, the primary pearlite nucleation sites occurred at grain boundaries, causing the grain size of the austenite to increase as the austenitization temperature increases [15]. This cooling time from austenitization temperature to room temperature corresponds to the final phase formation after employing different cooling media.

3.2 Microstructure Analysis

Based on Figure 4(a), the as-received microstructure of tested steel consists of a ferrite

phase12 (light area) and pearlite (black area) with a 9.199-GSN (grain size number) equivalent to 13.23 μm [10].

received sample. It is concluded that the grain size depends on the cooling rate. The full martensite was formed when water quench was

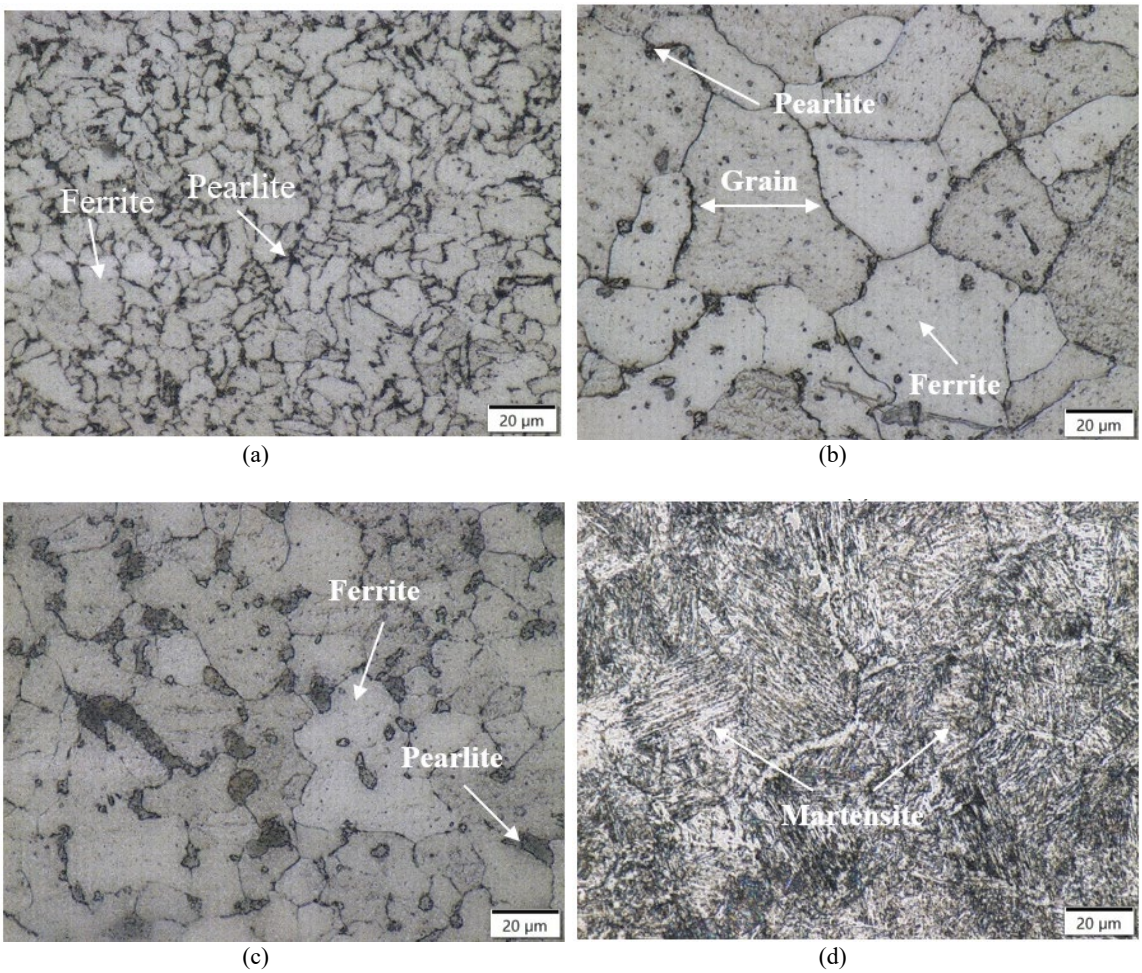

Figure 4. Microstructure of low carbon steel (a) as-received and after austenitizing at 920 °C with (b) furnace cooling, (c) air cooling, and (d) water quench

The microstructure evolution during the austenitization process at 920 ℃ for 30 minutes and subsequently cooled in different media is shown in Figures 4(b)-4(d). The cooling media used is furnace cooling, open-air cooling, and water cooling, which is used to generate different structures before intercritical anneal.

By heating at 920 ℃ for 30 minutes, the ferrite and pearlite transformed into an austenite phase. A significant phase transformation did not take place by furnace cooling (Fig. 4(b)), and only grain coarsening occurs to 6.2147 GSN (37.25 μm). The volume fraction of ferrite and pearlite is 82.81% and 17.19%, respectively. The open-air cooling does not trigger the phase transformation; therefore, the final phase remains ferrite (71.95%) and pearlite (29.05%) (Fig. 4(c)). After the air cooling process, the grain size (27.74 μm) is smaller than those processed by furnace cooling but still larger than the as-applied after austenitization (Fig. 4(d)). This result is in good agreement with the TTT diagram (Fig. 3), which was obtained by JMatPro software.

After getting the different initial structure, the intercritical annealed process was carried out at a temperature of 750 °C for 10 minutes, followed by quenching water. Figure 6 depicts the DP microstructures after intercritical annealed at 750 ℃, which transformed from the corresponding microstructure in Fig. 5. The dual-phase structure was obtained in all samples. In the furnace cooling + intercritical annealed sample, the smaller grain of the martensite phase can be seen with 18.36 vol.% in the grain boundary of ferrite (Fig. 5(a)). By heating in intercritical zone, the austenite was nucleated at the ferrite-pearlite interface and grew later until the pearlite transformation was completed. Because austenite nucleation is competitive in

recrystallized ferrite grains, it favors generating austenite networks, which subsequently transform into martensite networks during the quenching process [15]. Conversely, air cooling produces more martensite (27.85%) with nearly uniform distribution and coarsen martensite than furnace cooling. The average grain size is 38.82 μm and 31.02 μm for furnaces and open-air cooling, respectively. This difference is attributed to the initial structure before intercritical annealing (Figs. 4(b)-4(c)), which has a more uniform amount of pearlite that transforms into austenite when it passes through the A_{C1} line [5]-[6].

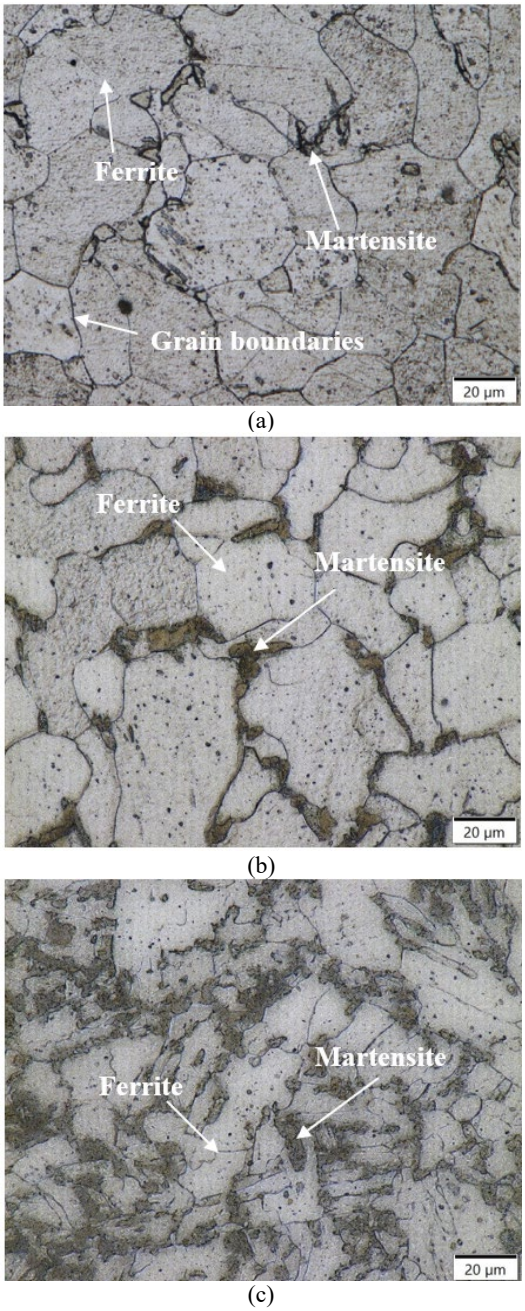

Figure 5. Microstructure after intercritical annealed with prior structure processed by (a) furnace cooling, (b) air cooling, and (c) water cooling

The intercritical annealing of the initial martensite structure produced by water quenching after austenitization generated a finer martensite than the other process (Fig. 5(c)). The amount of final martensite is higher (39.25%), and the average grain size is smaller (21.975 μm) of material water cooling + IA. When a prior-quenched structure is subjected to intercritical annealing, the martensite as a metastable phase has a driving energy to revert to its stable form and nucleate the austenite and fresh ferrite along the prior martensite boundary [1]. Furthermore, rapid cooling will transform the newly austenite into fresh martensite. It can be concluded that the phenomena are similar to the martemper process, which occurs in the suppression of carbide deposition and leads to the ferrite and martensite as the final structure [12].

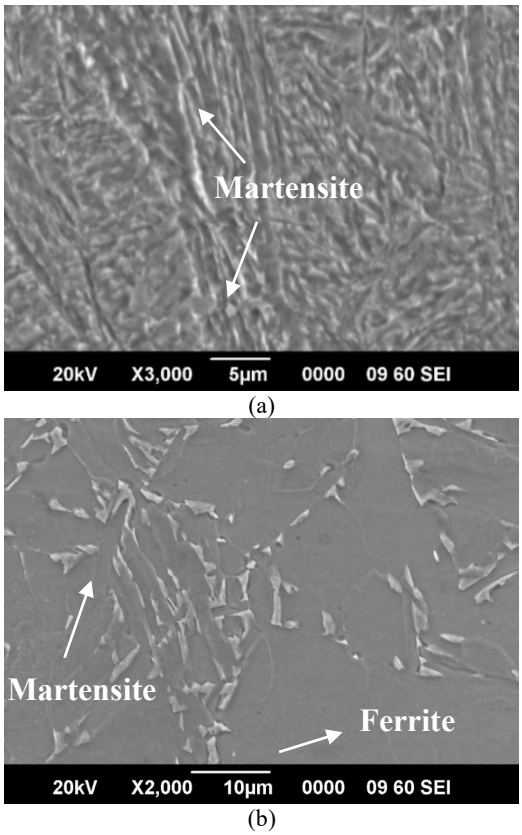

Figure 6. SEM image of quenched structure (a) before and (b) after intercritical annealed

The SEM (scanning electron microscope) image regarding the martensite structure before and after IA resulting from water quenching is shown in Figure 6. The full martensite after water quenching is visible with higher density (Fig. 6(a)) than after the intercritical annealing (Fig. 6(b)).

These results agree with the optical image, which shows another phase as ferrite after intercritical annealing. The fresh martensite is significantly smaller and shorter, less than 10μm.

More details of all the values of GSN, grain diameter, and phase fraction present in tested steel before and after the intercritical annealing process are presented in Table 3.

Table 3. Value of GSN, grain diameter, and phase fraction of tested steel before and after intercritical annealing

Code	GSN	Grain ⌀ (µm)	Phase Fraction (%)		
			Ferrite	Pearlite	Martensite
As-received	9.20	13.23	75.70	24.30	---
Furnace cooling	6.21	37.25	82.81	17.19	---
Open air cooling	7.31	27.74	70.95	29.05	---
Water cooling	---	12.27	---	---	100
Furnace cooling+IA	6.09	38.82	81.64	---	18.36
Open air cooling+IA	6.74	31.02	72.15	---	27.85
Water cooling+IA	7.74	21.97	60.75	---	39.25

3.3 Tensile Analysis

All specimens were subjected to a tensile test to confirm the stress-strain behavior under the applied tensile force, as shown in Figs. 7-8.

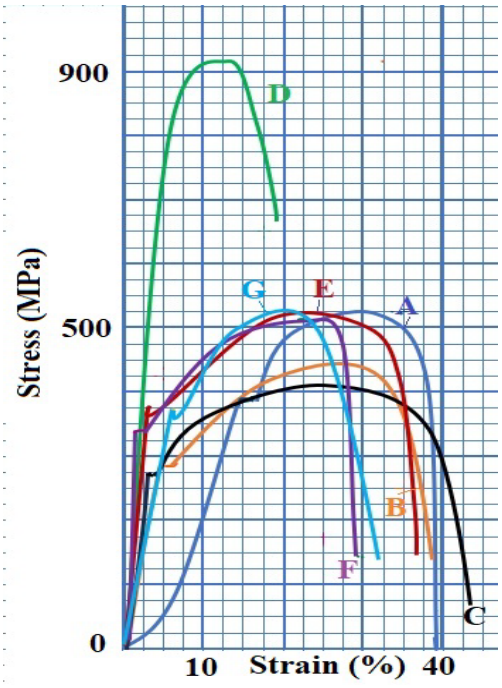

Figure 7. Tensile test results in tested steel (A = as-received; B = open-air cooling; C = Furnace cooling; D =. water cooling; E =. open air cooling+IA; F = furnace cooling + IA; G.= water cooling +IA)

Based on Figures 7-8, the as-received sample, consisting of a ferrite-pearlite structure, has 519 MPa of tensile strength and 39.2% elongation. The tensile properties after austenization vary depending on the cooling media. The tensile and yield strength increased as the cooling rate increased, considering grain size refinement followed the Hall-Petch relationship [16]. The UTS/YS (ultimate tensile strength yield strength) ratio decreased with the rising cooling rate up to 1.08. Rapid cooling in water medium obtained the highest tensile strength, ~919 MPa. Conversely, increasing tensile strength (Fig. 8(a)) is followed by decreasing elongation to 16.6% (Fig. 8(b)) as a consequence of complete martensite formation. Rapid cooling rates didn't give time for carbon diffusion into BCC (body-centered cubic) crystal, so the BCT (body-centered tetragonal) with high atomic packing density was formed during transformation. In addition, cooling in the furnace occurs more slowly than in the open air. This causes the grains in the furnace cooling to be larger, which causes them to become more ductile. As mentioned in the previous research, DP (dual phase) steels' stress-strain depicts low yield strength, continuous yielding, and high strain hardening [1].

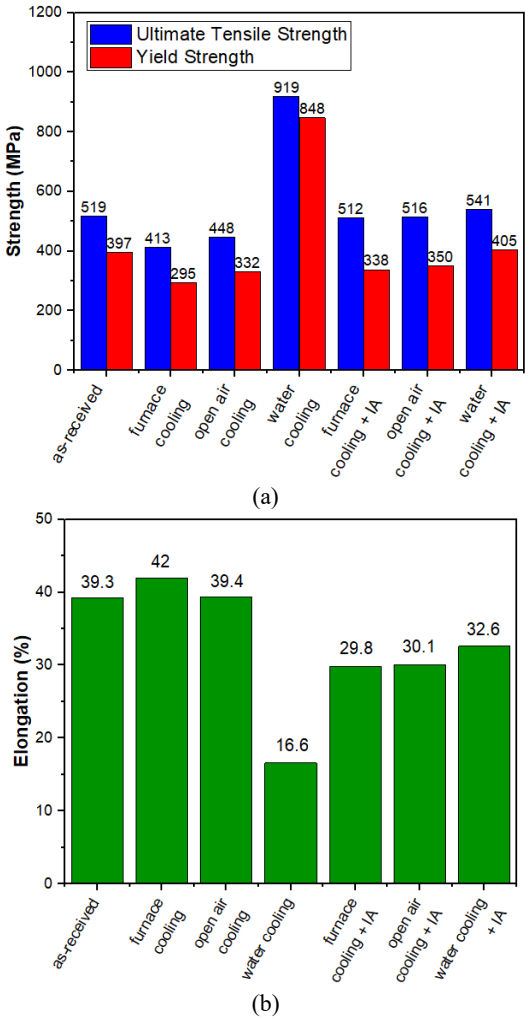

Figure 8. (a) Ultimate tensile and yield strength (b) elongation on low carbon steel before and after heat treatment + IA processing

Additionally, the dual-phase structure shows elongation maintenance around 29.8-32.6%,

although it has a brittle martensite structure (Fig 8(b)). As the cooling rate before the intercritical process increases, the tensile strength elongation improves up to 541 MPa, corresponding to the increased volume fraction of martensite (~39.25 vol.%, see Fig. 5(c)). Due to the shear and volume changes between austenite and martensite, it is expected that some unpinned dislocation in the surrounding of prior ferrite occurred and prevented yielding phenomenon, lead to a higher tensile strength [17]. Besides that, the different volume fractions and sizes of martensite in DP structures are also related to the strength and elongation of DP. More martensite volume fraction with uniform distribution as ferrite network provides higher UTS x ε properties.

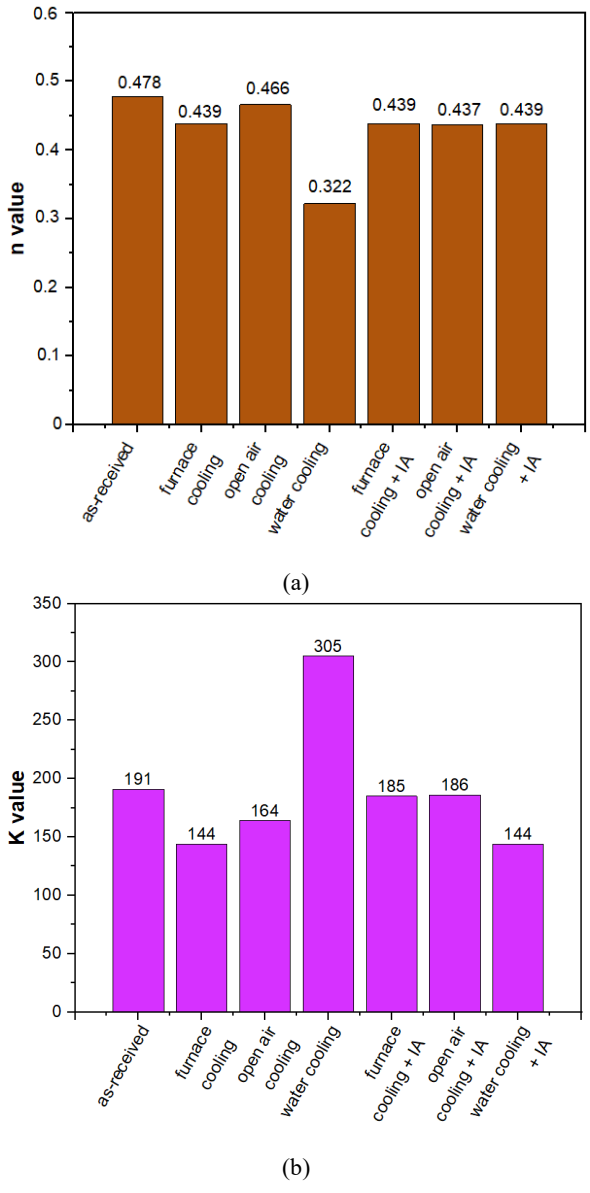

Figure 9. Tensile test results (a) n value and (b) K value in carbon steel before and after HT and IA processes

The strain hardening corresponding to the tensile curve is shown in Figure 9, represented by the work hardening exponent (n) and K values (Eq. 5).

The high strain hardening value indicates the possibility of deforming before instability and stretch before necking starts [1],[18]. For the ferritic-pearlite steel, the as-received steel has an the n value of 0.478 and the K value of 191.22. After austenitized at 920 °C, n value becomes lower, and K value becomes higher, resulting in the increasing cooling rate.

At the fully brittle martensite phase, the n value was lower (0.322) than the others, indicating the most insufficient work hardening due to the small area for plastic deformation. The strain hardening exponent slightly decreased around 0.437-0.439 after intercritical annealing, suggesting the dual-phase structure (ferrite + martensite) provides a similar behavior with other (ferrite+pearlite phase as a result of the furnace and open-air cooling). The work hardening rate of ferrite+martensite structure consists of three stages: (1) the initial gradient of ferrite glide was caused by moving dislocation, (2) the normal ferrite work hardening and constrained by martensite, and (3) co-deformation of both hardened ferrite and martensite [6],[15]. Zhao et al., [19] reported that the higher strain hardening occurred at initial plastic deformation due to the initial high density of free dislocation and the multiplication of dislocation in further strain. Nevertheless, the restraining ferrite deformation by martensite caused the decreasing strain hardening value. The work hardening rate of DP steels can be related to the function of volume fraction and particle size of martensite [17].

The prior water-quenched structure provide a higher strain hardening value of ~0.439, indicating the higher strain hardening ability of martensite tempered. This can be attributed to the uniform distribution of network martensite surrounding ferrite grain and fine grain of martensite (Figs. 5(c) and 6(b)), similar to Deng et al., result [16].

3.4 Hardness Test

The complete results of the hardness test with the Vickers method are shown in Figure 10. The results of the as-received material hardness test were 180 HV, whereas, after processing in the furnace and air, there was a decrease, namely 158 and 168 HV. This was due to the increase in grain size, making it softer. The quenching result in water shows an increase with a high hardness value, namely 347 HV. This indicates that the material becomes hard due to the dominance of the martensite phase.

The intercritical annealing increased in the material's hardness compared to the as-received state, namely 183 and 186, and 199 Hv for the specimens cooled in the furnace, air, and water, respectively.

Because the initial structure persists in ferrite and pearlite before intercritical annealing, the hardness due to the furnace and open-air cooling is lower than that of water cooling. The full martensite as the initial structure provided a high martensite volume fraction of ~ 39.25% after intercritical annealing. When heated again in the intercritical annealing zone, some of the martensite phase returns to the ferrite, although there is still martensite left and new martensite is formed. The martensite transformation induced by intercritical annealing caused a decrease in hardness (from 347 HV to 199 HV).

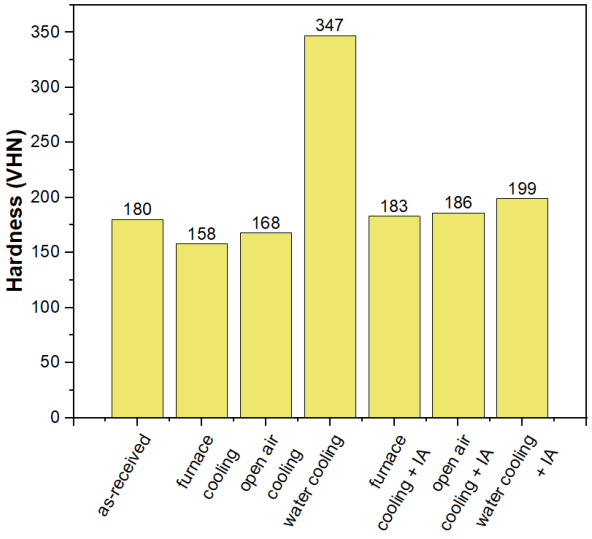

Figure 10. Vickers hardness test results of tested steel

4. CONCLUSION

In this work, the different cooling rates from austenitization lead to the other initial structures of low-alloy carbon steel before intercritical annealing. The other initial structures, in turn, resulted in dual-phase steel with different microstructure and mechanical properties following the intercritical annealing. The slower cooling (with furnace and open-air cooling) provides the pearlite + ferrite as the initial structure, whereas the rapid cooling generates the martensite structure. As the cooling rate increased, the tensile strength increased to ~919 MPa, and the elongation decreased to ~16.6%. During intercritical annealing, the pearlite was transformed into austenite after passing the AC1 temperature and led the austenite network near recrystallized ferrite with 38.817 μm of grain size. As the ferrite-martensite phase, the water-quenched structure provides the uniformly finer martensite of less than 10 μm, correlating the higher tensile strength (541 MPa), more elongation (32.6%), and higher hardness (199 VHN). Nevertheless, the differences in initial structure have an insignificant effect on strain-hardening behavior.

ACKNOWLEDGMENT

Thank you to the Metallurgical Research Center - National Research and Innovation Agency, which has funded this research.

REFERENCES

[1] M. Soliman and H. Palkowski, "Strain hardening dependence on the structure in dual-phase steels," *Steel Res. Int.*, vol. 92, no. 4, pp. 1-15, 2021. Doi: 10.1002/srin.202000518.

[2] J. Samei, Y. Salib, M. Amirmaleki, and D. S. Wilkinson, "The role of microstructure on edge cracks in dual phase and quench and partitioning steels subject to severe cold rolling," *Scr. Mater.*, vol. 173, pp. 86-90, 2019. Doi: 10.1016/j.scriptamat.2019.08.012.

[3] T. Yalçinkaya, S. O. Çakmak, and C. Tekoğlu, "A crystal plasticity based finite element framework for RVE calculations of two-phase materials: Void nucleation in dual-phase steels," *Finite Elem. Anal. Des.*, vol. 187, pp. 103510, 2021. Doi: 10.1016/j.finel.2020.103510.

[4] A. Kalhor, M. Soleimani, H. Mirzadeh, and V. Uthaisangsuk, "A review of recent progress in mechanical and corrosion properties of dual phase steels," *Arch. Civ. Mech. Eng.*, vol. 20, no. 3, pp. 1-14, 2020. Doi: 10.1007/s43452-020-00088-0.

[5] A. Kalhor and H. Mirzadeh, "Tailoring the microstructure and mechanical properties of dual phase steel based on the initial microstructure," *Steel Res. Int.*, vol. 88, no. 8, pp. 1-8, 2017. Doi: 10.1002/srin.201600385.

[6] F. Jamei, H. Mirzadeh, and M. Zamani, "Synergistic effects of holding time at intercritical annealing temperature and initial microstructure on the mechanical properties of dual phase steel," *Mater. Sci. Eng. A*, vol. 750, pp. 125-131, 2019. Doi: 10.1016/j.msea.2019.02.052.

[7] J. Adamczyk, and A.Grjcar "Heat treatment and mechanical properties of low-carbon steel with dual-phase

microstructure," *Journal of Achievement in Materials and Manufacturing Engineering,* vol. 22, no. 1, 2007.

[8] H. Dannoshita, T. Ogawa, K. Maruoka, and K. Ushioda, "Effect of initial microstructures on austenite formation behavior during intercritical annealing in low-carbon steel," *Mater. Trans.*, vol. 60, no. 1, pp. 165-168, 2019. Doi: 10.2320/matertrans.M2018298.

[9] M. Maleki, H. Mirzadeh, and M. Zamani, "Effect of intercritical annealing time at pearlite dissolution finish temperature (Ac1f) on mechanical properties of low-carbon dual-phase steel," *J. Mater. Eng. Perform.*, vol. 28, no. 4, pp. 2178-2183, 2019. Doi: 10.1007/s11665-019-04009-y.

[10] M. Maleki, H. Mirzadeh, and M. Zamani, "Effect of intercritical annealing on mechanical properties and work-hardening response of high formability dual phase steel," *Steel Res. Int.*, vol. 89, no. 4, pp. 1-7, 2018. Doi: 10.1002/srin.201700412.

[11] ASTM International, "Standard test methods for determining average grain size," E 112-12, 2010. Doi: 10.1520/E0112-12.1.4.

[12] J. Adamczyk and A. Grajcar, "Heat treatment and mechanical properties of low-carbon steel with dual-phase microstructure manufacturing and processing," *J. Achiev. Mater. Manuf. Eng.*, vol. 22, no. 1, pp. 13-20, 2007.

[13] N. Lanzillotto and F. B. Pickering, "Structure-property dual-phase steels relationships in," *Met. Sci.*, vol. 16, no. August, pp. 371-382, 1982.

[14] M. A. M. Gurgel, E. S. B. Junior, R. S. Teixeira, G. O. Nascimento, S. S. Oliveira, D. N. F. Leite, L. P. Moreira, L. P. Brandao, and A. S. Paula , "Microstructure and continuous cooling transformation of an Fe-7.1Al-0.7Mn-0.4C-0.3Nb Alloy," *Metals (Basel).*, vol. 12, no. 8, pp. 1-16, 2022. Doi: 10.3390/met12081305.

[15] P. D. Basoeki, "Effects of DP steel microstructure on the disappearance of discontinuous yielding," *MATEC Web Conf.*, vol. 204, pp. 1-8, 2018. Doi: 10.1051/matecconf/201820407013.

[16] Y. G. Deng, H. S. Di, and R. D. K. Misra, "On significance of initial microstructure in governing mechanical behavior and fracture of dual-phase steels," *J. Iron Steel Res. Int.*, vol. 25, no. 9, pp. 932-942, 2018. Doi: 10.1007/s42243-018-0133-0.

[17] H. Mirzadeh, M. Alibeyki, and M. Najafi, "Unraveling the initial microstructure effects on mechanical properties and work-hardening capacity of dual-phase steel," *Metall. Mater. Trans. A Phys. Metall. Mater. Sci.*, vol. 48, no. 10, pp. 4565-4573, 2017. Doi: 10.1007/s11661-017-4246-z.

[18] Y. Mazaheri, A. Kermanpur, and A. Najafizadeh, "A novel route for development of ultrahigh strength dual phase steels," *Mater. Sci. Eng. A*, vol. 619, pp. 1-11, 2014. Doi: 10.1016/j.msea.2014.09.058.

[19] Z. Zhao, T. Tong, J. Liang, H. Yin, A. Zhao, and D. Tang, "Microstructure, mechanical properties and fracture behavior of ultra-high strength dual-phase steel," *Mater. Sci. Eng. A*, vol. 618, pp. 182-188, 2014. Doi: 10.1016/j.msea.2014.09.005.